Carbohydrate Polymers 111 (2014) 576–583

Contents lists available at ScienceDirect

Carbohydrate Polymers

journal homepage: www.elsevier.com/locate/carbpol

Extraction, preliminary characterization and immunostimulatory activity *in vitro* of a polysaccharide isolated from *Strongylocentrotus nudus* eggs

Yihua Ma, Yingying Xing, Huiwen Mi, Zhenquan Guo, Yuanyuan Lu*, Tao Xi*

Department of Marine Pharmacy, China Pharmaceutical University, Nanjing, Jiangsu 210009, China

ARTICLE INFO

Article history:
Received 19 December 2013
Received in revised form 31 March 2014
Accepted 3 April 2014
Available online 18 April 2014

Keywords:
Sea urchin
SEP-2
Response surface methodology
Characterization
Immunostimulatory activity

ABSTRACT

A new water-soluble polysaccharide (SEP-2), with a molecular weight of 6.78×10^5 Da, was isolated from *Strongylocentrotus nudus* eggs under the extraction conditions optimized by response surface methodology (RSM). Preliminary characterization of SEP-2 was performed by HPSEC and GC–MS, indicating that SEP-2 could be a D-glucan containing a (1 → 4)-linked D-Glcp backbone with (1 → 3)-linked D-Glcp side chains. In subsequent immunostimulatory studies, significantly enhanced ROS level, NO production and inflammatory cytokines secretion (IL-1β, IL-6, and TNF-α) were observed in SEP-2 treated murine macrophage cell line RAW264.7. These results suggest that SEP-2 might have the capability to enhance the microbicidal activity and killing function of macrophages through the polarization toward the pro-inflammatory M1 state.

1. Introduction

Sea urchins, belonging to the phylum echinoderm, are regarded as seafood delicacy for their wonderful flavor and high nutritional value in China. In Traditional Chinese Medicine, the roes or eggs of sea urchins are termed "Yun Dan" and used for curing precordial pain, preventing atherosclerosis and enhancing immunity. However, there is very limited literature on the polysaccharides from *Strongylocentrotus nudus* eggs and their bioactivities.

In the last few decades, polysaccharides isolated from microorganism, plants and animals have been the focus of much attention in the fields of biochemistry and pharmacology due to their broad spectrum of therapeutic properties, relative low toxicity and limited side effects (Chihara, 1992; Ramberg, Nelson, & Sinnott, 2010). One of the primary mechanisms involved in the activities of polysaccharides occurs *via* the modulation of macrophage function (Schepetkin & Quinn, 2006). In addition, a diverse range of polysaccharides have potential to increase macrophage cytotoxic activity, activate phagocytic activity, induce reactive oxygen species (ROS) and nitric oxide (NO) production, and enhance secretion of cytokines and chemokines, such as tumor necrosis factor (TNF-α), interleukin (IL)-1β, IL-6, IL-8 and interferon (IFN)-γ (Cheng, Wan, Wang, Jin, & Xu, 2008; Schepetkin et al., 2008).

In our previous study, two completely separated fractions were found in *S. nudus* eggs. The main fraction, *S. nudus* eggs polysaccharide (SEP), which was successfully isolated and well characterized, has already been proven to be a potent immunomodulatory agent (H. Wang et al., 2011; Liu et al., 2007, 2008; M. Wang et al., 2011). Therefore, the isolation and evaluation of the other polysaccharide with smaller molecular weight (SEP-2) provide a great opportunity for the discovery of potential immunomodulatory agent.

Here, the extracting parameters were optimized using Response Surface Methodology (RSM) to effectively isolate SEP-2 from *S. nudus* eggs. The physicochemical properties of purified SEP-2 were preliminarily investigated by HPSEC and GC–MS. Furthermore, the immunostimulatory activity of SEP-2 was evaluated by measuring the production of IL-1β, IL-6, TNF-α, NO and ROS on murine macrophage cell line RAW264.7.

2. Materials and methods

2.1. Materials and chemicals

Dalian purple sea urchins were collected from Huanghai Sea, China. Shell, spines and intestine were immediately removed, and the eggs were stored at −20 °C. Murine macrophage cell

* Corresponding authors. Tel.: +86 25 83271022; fax: +86 25 83271249.
E-mail addresses: mada1986@126.com (Y. Ma), xingying1980@126.com (Y. Xing), wenwen_3150@126.com (H. Mi), guoquan5001@163.com (Z. Guo), luyy626@163.com (Y. Lu), xitao18@hotmail.com, xitaocpu@hotmail.com (T. Xi).

http://dx.doi.org/10.1016/j.carbpol.2014.04.010
0144-8617/

line RAW264.7 was obtained from Cell Culture Center of Chinese Academy of Medical Sciences (Beijing, China). Papain, lipopolysaccharides from *Escherichia coli* 0111: B4 (LPS), 2′,7′-dichlorofluorescein diacetate (DCFH-DA), standard dextrans and Griess reagent were purchased from Sigma–Aldrich Co. (St. Louis, MO, USA). Dulbecco's modified Eagle's medium-high glucose (DMEM), fetal bovine serum (FBS), streptomycin and penicillin were all purchased from Gibco Laboratories (Grand Island, NY, USA). TRIzol reagent, IL-1β, IL-6 and TNF-α mouse sandwich-based enzyme-linked immunosorbent assay (ELISA) kits were purchased from Invitrogen (Carlsbad, CA, USA). ImProm-II reverse transcription system was purchased from Promega Co. (Madison, WI, USA). All other chemicals were of analytical grade.

2.2. Extraction and isolation of SEP-2

2.2.1. Extraction procedures

In brief, 200 g sea urchin eggs were treated with 200 mL acetone three times to remove fat and pigments. Then the defatted deposit was collected and vacuum dried for 16 h at 50 °C to constant weight. The pretreated samples (10 g) were extracted with 100 mL distilled water at a designated extraction temperature and extraction time. The supernatants were then collected by centrifugation and concentrated *in vacuo*, and then deproteinated using a combination of papain enzymolysis and Sevag method. Crude polysaccharide was precipitated upon the addition of designated levels of ethanol and incubated overnight at 4 °C. The content of SEP-2 was analyzed by high performance liquid chromatography (HPLC) (Waters 600, TSK gel 4000 PWXL column, 2414 refractive index detector) using peak area normalization method.

2.2.2. Box–Behnken design

To improve the content of SEP-2 in crude polysaccharide, three independent variables (X_1, extraction temperature, °C; X_2, extraction time, h; X_3, ratio of ethanol to supernatant) at three levels were selected for response surface methodology of Box–Behnken design (BBD). The content of SEP-2 in crude polysaccharide (Y, %) was taken as the response for the combination of the independent variables. Design-Expert software (version 7.0) was employed to analyze the experimental data and estimate the response of the independent variables. Statistical significance of the model equation was determined by Fisher's test (Fisher, 1922).

2.3. Preliminary characterization of SEP-2

2.3.1. Homogeneity and molecular weight of SEP-2

The homogeneity and molecular weight of SEP-2 was determined *via* high-performance gel-permeation chromatography (HPGPC) using a LC-10AD HPLC system (Shimadzu Co. Ltd., Japan) equipped with SB-804 HQ and SB-802 HQ (Shodex OHpak, Japan) columns connected in series and a refractive index detector. Elution was performed with 0.15 M $NaNO_3$ at a flow rate of 0.5 mL/min and the column temperature maintained at 30 °C. Dextrans (0.2%, w/v) with different molecular weights (708, 375, 200, 47.1, 21.1, 9.6 and 0.18 kDa) were used as standards for calibration. The molecular weight of SEP-2 was estimated using Shimadzu LCsolution GPC software.

2.3.2. Detection of LPS contamination of SEP-2

LPS contamination in SEP-2 was determined in order to ensure the specificity of the subsequent immunostimulatory studies. The LPS standard from *E. coli* 0111:B4 (0.5 mg) was sonicated in deionized water and then dried under a N_2 stream. The residue was dissolved in 400 μL MeOH and subjected to methanolysis by the addition of 100 μL of 3 M MeOH–HCl. The mixture was sealed and kept at 80 °C for 20 h. The solution was then partitioned between hexane and deionized water and the hexane phase was evaporated under a gentle N_2 stream. The residue was acetylated with Ac_2O–pyridine (1:1, v/v; 500 μL) at 100 °C for 1 h. Serial dilutions of the acetylated product were then prepared, using acetone as solvent, corresponding to concentrations of 50, 25, 12.5, 6.25, and 3.125 ng of LPS, which were analyzed by GC–MS. 3-OAc-$C_{14:0}$ methyl ester was chosen as the chemical marker for LPS to get a standard curve of LPS concentration *vs.* integrated area of the extracted-ion chromatograms. SEP-2 (2 mg) was diluted in deionized water and an aliquot containing 0.3 mg of SEP-2 was then collected, the procedure being that described above up to the acetylation step. The sample was gently evaporated under a N_2 stream, and dissolved in acetone (5 μL), concentrated down to 1 μL, then subjected to GC–MS analysis (Santana-Filho et al., 2012).

2.3.3. Monosaccharide composition

SEP-2 (5 mg) was hydrolyzed with 2 M trifluoroacetic acid (TFA) at 100 °C for 8 h, followed by evaporation to dryness. The hydrolyzed product was successively reduced with $NaBH_4$ (1 mg) and acetylated with Ac_2O–pyridine (1:1, v/v; 500 μL) at 100 °C for 30 min. The identification and quantification of alditol acetates were performed using a Varian 3400 gas chromatograph (Hewlett-Packard Component, USA) linked to flame-ionization detector (FID). A capillary column (30 m × 0.25 mm × 0.25 μm) of HP-5 was used for analysis and N_2 was employed as the carrier gas. The temperature program was set to be increased from 160 to 210 °C at 2 °C/min, then to be kept at 210 °C for 8 min, and finally to be increased to 240 °C at 5 °C/min and kept for 6 min at the final temperature. The standard monosaccharides were measured using the same procedure.

2.3.4. Methylation analysis of SEP-2

Methylation analysis of SEP-2 was performed according to the modified Hakomori method (Ciucanu & Kerek, 1984). In brief, purified SEP-2 (10 mg) was methylated using powdered NaOH in DMSO–MeI. The completion of methylation was determined by the disappearance of OH bands in FTIR spectroscopy. The methylated derivatives were hydrolyzed with 2 M TFA at 110 °C for 6 h followed by $NaBH_4$ reduction and Ac_2O–pyridine acetylation as mentioned above. The derivatized products were extracted, evaporated and redissolved in 100 μL $CHCl_3$, then analyzed by gas chromatography–mass spectrometry (GC–MS) on a HP6890II/5975 instrument (Agilent Technologies Co. Ltd., USA) using a DB 225 fused silica capillary column (0.25 mm × 30 m). The O-methylated alditol acetates were identified by their typical mass fragmentation patterns and retention times (Bi et al., 2009; Cordeiro, Reinhardt, & Iacomini, 2012). The results are expressed as a relative percentage of each component.

2.4. Activation of RAW264.7 macrophages in vitro

2.4.1. Cell culture

The murine macrophage cell line RAW264.7 was maintained in DMEM medium containing 10% heat-inactivated FBS, 100 μg/mL streptomycin and 100 U/mL penicillin at 37 °C under a humidified atmosphere of 5% CO_2.

2.4.2. Reverse transcription-polymerase chain reaction (RT-PCR)

The RAW264.7 cells were cultured in the presence of SEP-2 at 0, 100, 200, 400 and 800 μg/mL for 12 h. Total RNAs were isolated using TRIzol reagent according to the manufacturer's instructions. For RT-PCR, single-stranded cDNA was synthesized from 2 μg of total RNA by using ImProm-II reverse transcription system.

The primer sequences used in this study were as follows:

for TNF-α, sense 5′-GGA TCT CAA AGA CAA CCA ACT AG-3′, anti-sense 5′-ACA GAG CAA TGA CTC CAA AGT AG-3′;
for IL-1β, sense 5′-ATG GCA ATG TTC CTG AAC TCA ACT-3′, anti-sense 5′-CAG GAC AGG TAT AGA TTC TTT CCT TT-3′;
for IL-6, sense 5′-CTT GCC CAA GCA GGC CAC AG-3′, anti-sense 5′-GAG CCT TAT GTG TTG TAA GC-3′;
for iNOS, sense 5′-CCT TCC GAA GTT TCT GGC AGC AGC-3′, anti-sense 5′-GGC TGT CAG AGC CTC GTG GCT TTG G-3′;
for GAPDH, sense 5′-ATT CAA CGG CAC AGT CAA GG-3′, anti-sense 5′-GCA GAA GGG GCG GAG ATG A-3′.

All the primers were designed based on published nucleic acid sequences available in the GenBank database. Each assay was run on Applied Biosystems 7300 Real-Time PCR system in triplicate and the expression fold-changes of products were analyzed using the comparative C_T method (Schmittgen & Livak, 2008).

2.4.3. Enzyme-linked immunosorbent assay (ELISA)

Cell culture supernatants were collected 24 h after SEP-2 treatment for cytokine analysis. The protein concentrations of IL-1β, IL-6, and TNF-α were measured using commercial ELISA kits according to the manufacturer's instructions.

2.4.4. Measurement of intracellular ROS generation

RAW264.7 cells were seeded at 3×10^5 cells/well in a 6-well plate and treated with 0, 100, 200, 400 and 800 μg/mL SEP-2, respectively, for 12 h. Then cells were incubated with 10 μM DCFH-DA in serum-free DMEM medium in the dark at 37 °C for 15 min. After incubation, cells from each treatment group were harvested and then subjected to BD FACSCalibur system for flow cytometric analyses after being resuspended in 500 μL PBS.

2.4.5. Nitrite assay

The nitrite concentration in the supernatant was measured as an indicator of NO production according to the Griess reaction (Granger, Taintor, Boockvar, & Hibbs, 1995). RAW264.7 cells were seeded at a density of 10^5 cell/well into a 24-well plate and treated with various concentrations (0, 100, 200, 400 and 800 μg/mL) of SEP-2 for 24 h. Supernatant was mixed with an equal volume of Griess reagent and incubated at room temperature for 15 min. Then the absorbance of the mixture was determined at 540 nm using a microplate reader. All measurements were performed in triplicate and the nitrite levels determined based on standard curves established with $NaNO_2$.

3. Results and discussion

3.1. Optimization of the extraction process

To increase the SEP-2 content in crude polysaccharide, the combined effect of the three variables (extraction temperature, extraction time and ethanol to supernatant ratio) was examined by employing a 17 runs Box–Behnken design (BBD). The BBD experimental plan and the values of response Y (content of SEP-2 in crude polysaccharide, %) under the different experimental combinations are presented in Table 1.

The empirical relationships between response and the tested variables were related by the following second-order polynomial equation:

$$Y = 21.46 - 3.82X_1 + 0.31X_2 - 0.4X_3 + 0.21X_1X_2 + 0.41X_1X_3 - 0.43X_2X_3 - 2.30X_1^2 - 1.20X_2^2 - 2.37X_3^2$$

where X_1, X_2, and X_3 are the test variables in terms of coded factors.

Table 1
Box–Behnken design and results of SEP-2 content in crude polysaccharide.

Run	X_1 (extraction temperature, °C)	X_2 (extraction time, h)	X_3 (ratio of ethanol to supernatant)	Y (content of SEP-2 in crude polysaccharide, %)
1	80	4	5:1	22.05
2	90	5	5:1	21.48
3	80	5	6:1	19.84
4	90	5	5:1	21.42
5	100	6	6:1	14.31
6	80	6	5:1	21.84
7	100	4	5:1	13.67
8	90	6	4:1	16.44
9	90	4	4:1	17.56
10	100	5	6:1	13.33
11	90	4	6:1	17.20
12	90	5	5:1	21.94
13	90	6	6:1	17.38
14	90	5	5:1	20.84
15	80	5	4:1	21.06
16	90	5	5:1	21.63
17	100	5	4:1	12.90

The results obtained by analysis of variance (ANOVA) for the model were shown in Table 2. The coefficient of determination (R^2) was 0.9916, indicating that only 0.84% of the total variations was not explained by the model. The F-value of 1.75 for the "lack of fit" was insignificant relative to the pure error indicating there was a chance of 29.57% that a lack-of-fit F-value this large could occur due to noise. A low value for the coefficient of variation (C.V.) (2.48%) clearly indicated a high degree of precision and reliability of the experimental values. Meanwhile, the statistical significance of each coefficient was determined by F-values and P-values. The linear coefficients (X_1 and X_3) and quadratic term coefficients (X_1^2, X_2^2 and X_3^2) were significant ($p < 0.05$), which implied that the extraction temperature and the ratio of ethanol to supernatant significantly affected the content of SEP-2 in crude polysaccharide.

According to the 3D response surfaces and 2D contour plots (Supplementary material, Fig. 1), the predicted optimum values of the test variables were 81.6 °C for extraction temperature, 5.09 h for extraction time, and 4.83:1 for the ratio of ethanol to supernatant, while the predicted SEP-2 content (23.117%) was in reasonable agreement with the experimental value of 23.21 ± 0.14%. For practical application, a set of modified optimal conditions (80 °C for extraction temperature, 5 h for extraction time, and 5:1 for the ratio of ethanol to supernatant) was tested, and a mean SEP-2 content of 22.78 ± 0.13% was obtained showing no statistical difference compared to the result of optimized conditions (Supplementary material, Table 1).

3.2. Preliminary characterization of SEP-2

3.2.1. Homogeneity, M_W and monosaccharide composition of SEP-2

Crude polysaccharide obtained under the modified optimal conditions was redissolved in distilled water and applied to DE52 (OH^-) anion exchange column eluting with a gradient of 0–0.1 M NaCl (Fig. 1a). The main peak of the DE52 chromatography (Tube 10–20) was collected and further fractionated on a Sephacryl S-400 column by eluting with 0.05 M NaCl at a flow rate of 30 mL/h to yield two completely separated fractions (Fig. 1b). The main fraction (Tube 18–24) was identified as SEP, and the other fraction (Tube 37–41) was collected, dialyzed and lyophilized to get purified SEP-2. The yield of SEP-2 from crude extracellular polysaccharide was about 15%.

SEP-2 appeared as white powder with no absorption at either 280 or 260 nm, which confirmed the absence of protein and nucleic

Table 2
Analysis of variance (ANOVA) for the response surface quadratic model.

Source	Sum of squares	df	Mean square	*F*-value	*p*-Value Prob > *F*	
Model	178.17	9	19.80	92.18	<0.0001	Significant
X_1-extraction temperature	116.92	1	116.92	544.36	<0.0001	
X_2-extraction time	0.78	1	0.78	3.63	0.10	
X_3-ratio of ethanol to supernatant	1.29	1	1.29	6.02	0.04	
X_1X_2	0.18	1	0.18	0.84	0.39	
X_1X_3	0.68	1	0.68	3.17	0.12	
X_2X_3	0.73	1	0.73	3.41	0.11	
X_1^2	22.33	1	22.33	103.98	<0.0001	
X_2^2	6.01	1	6.01	28.00	0.0011	
X_3^2	23.74	1	23.74	110.51	<0.0001	
Residual	1.50	7	0.21			
Lack of fit	0.85	3	0.28	1.75	0.30	Not significant
Pure error	0.65	4	0.16			
Cor total	179.68	16				

Std. dev.	0.4634	R^2	0.9916
Mean	18.6997	Adj R^2	0.9809
C.V. %	2.4783	Pred R^2	0.9184
PRESS	14.6564	Adeq precision	25.1395

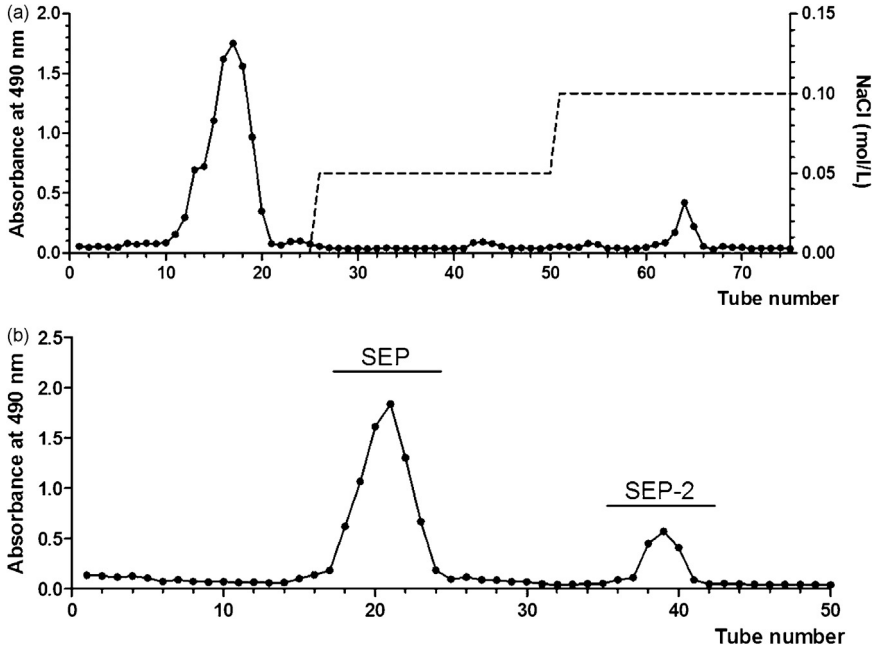

Fig. 1. Purification of SEP-2 from *Strongylocentrotus nudus* eggs. (a) Elution profile on DE52 anion exchange column. (5.0 cm × 40 cm) with step wise 0–0.1 M NaCl eluent. (b) Elution profile on Sephacryl S-400 column (1.0 cm × 60 cm) with 0.05 M NaCl eluent.

acid in SEP-2. A standard curve of LPS concentration *vs.* integrated area of the extracted-ion chromatograms was obtained with a high R^2 of 0.986 (Supplementary material, Fig. 2), and no *m/z* 257 or other characteristic ions of 3-OAc-$C_{14:0}$ methyl ester was detected indicating there was no LPS contamination in SEP-2.

The HPGPC profile of SEP-2 (Fig. 2) showed a single and symmetrical peak at 29.054 min with a purity of 98.51%. The average molecular weight of SEP-2 was 6.78×10^5 Da.

The monosaccharide composition of SEP-2 was analyzed by GC and the result indicated that D-glucose was the only ingredient of SEP-2 (Supplementary material, Fig. 3).

3.2.2. Methylation analysis of SEP-2

In order to determine the position of the glycosidic linkage, SEP-2 was methylated by modified Hakomori method. The O-methylated alditol acetate of SEP-2 was prepared and subjected to GC–MS, and the ratios of the linkages present were listed in Table 3. Large amounts of 2,3,6-Me_3-Glc and 2,4,6-Me_3-Glc suggested the existence of (1→4)-linked and (1→3)-linked D-glucose units. The detected 2,6-Me_2-Glc and 2,3,4,6-Me_4-Glc suggested that small amounts of (1→3,4)-linked D-glucose and (1→) D-glucose residues were contained. The presence of

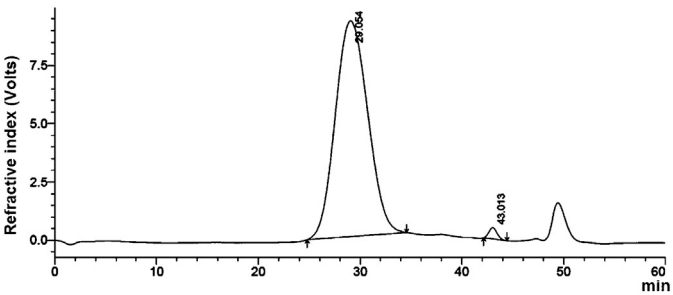

Fig. 2. Elution profiles of SEP-2 determined by HPSEC using refractive index detectors, and 0.15 M $NaNO_3$ as eluent.

Table 3
Methylalditol acetates formed on methylation analysis of SEP-2.

Methylated alditol acetates	Rt (min)	% area of fragments	Linkage type
2,3,4,6-Me_4-Glc	12.263	6.09	D-Glcp-(1→
2,3,6-Me_3-Glc	14.439	56.75	→4)-D-Glcp-(1→
2,4,6-Me_3-Glc	13.725	30.77	→3)-D-Glcp-(1→
2,6-Me_2-Glc	14.652	6.39	→3,4)-D-Glcp-(1→

2,3,4,6-Me_4-Glc = 1,5-di-O-acetyl-2,3,4,6-tetra-O-methyl-D-glucitol, *etc.*

2,3,4,6-Me_4-Glc, 2,3,6-Me_3-Glc, 2,4,6-Me_3-Glc and 2,6-Me_2-Glc detected in molar ratio of 1:9:5:1 indicated that SEP-2 could consist of a (1→4)-linked D-glucose backbone with (1→3)-linked D-glucose branches on position O-3. Moreover, the (1→4)-linked D-glucose main chain was confirmed by smith degradation and partial hydrolysis (Kumirska et al., 2008) (Data not shown). These data reflect that the linkage pattern of the polysaccharide SEP-2 was different from the other polysaccharides SEP isolated from purple sea urchin eggs (Liu et al., 2007).

3.3. Activation of macrophages by SEP-2 in vitro

Macrophages are the first line of defense against microbial invaders and malignancies by the secretion of inflammatory mediators including cytokines, chemokines and nitric oxide. Activation of macrophages is a key event in innate and adaptive immunity for initiation and propagation of defensive reactions against pathogens. There are literatures reporting the immunomodulatory activity of polysaccharides, and prior studies on SEP have already revealed its activation effects on macrophages (Devi et al., 2013; Liu et al., 2008; Zhang et al., 2013). Inspired by these compelling results, the effect of SEP-2 on murine macrophage cell line RAW264.7 was investigated *in vitro*.

3.3.1. SEP-2 up-regulates NO production and iNOS expression in RAW264.7 macrophages

Nitric oxide (NO) is a small free radical generated by a family of nitric oxide synthases (NOS) *via* the oxidative deamination of L-arginine. NO has multiple physiologic and pathophysiologic functions due to its wide distribution and its involvement of diverse biological mechanisms (Kadowaki et al., 2013). More importantly, in macrophages, the production of NO *via* iNOS is crucial for killing tumor cells, infected cells and some pathogens (Jiang, Okimura, Yamaguchi, & Oda, 2011). The toxic effects of NO and its derivatives on target cells are due to several known mechanisms, including inactivation of iron–sulfur cluster containing enzymes (Drapier & Hibbs, 1988), inhibition of DNA-binding activity of zinc finger-type transcriptional factors (Kroncke et al., 1994) and destruction of the mitochondrial membrane potential (Richter, Gogvadze, Schlapbach, Schweizer, & Schlegel, 1994).

To evaluate the effects of SEP-2 on NO production and iNOS expression in RAW264.7 macrophage cells, Griess assay and RT-PCR analysis were applied to determine the nitrite accumulation and iNOS mRNA level respectively. As shown in Fig. 3a, upon stimulation with SEP-2, NO production increased dose-dependently to an approximate value of 31.03 μM, which was 11-fold compared to the level detected in the control group (2.78 μM). Correspondingly, the mRNA level of iNOS increased 1.92 to 17.17-fold after treatment with SEP-2 at concentrations ranging from 100 to 800 μg/mL in a dose-dependent manner (Fig. 3b). Given the above, these results suggest that SEP-2 probably increases NO production *via* the upregulation of iNOS expression at transcriptional level in RAW264.7 cells. There are literatures reporting the polysaccharides could trigger the protein kinase C or MAPK signaling pathway and activate the transcription factors such as NF-κB and AP-1 by binding to the Toll-like receptor (TLR) on the surface of macrophages (Li, Yan, Brauner, & Tullus, 2002; Meena et al., 2013; Wang et al., 2012), which provided a theoretical basis for investigating the detailed mechanism of SEP-2 on the NO production in RAW264.7 cells.

3.3.2. SEP-2 induces intracellular generation of ROS

Reactive oxygen species (ROS) synthesized by NADPH oxidase act as secondary messengers in many cellular processes, including signal transduction, redox signaling, autophagy and respiratory burst (Lee & Yang, 2012). In macrophages, ROS is a key functional feature of the differentiation, activation and function. A consequence of heightened ROS synthesis is activation of the MAPKs and NF-κB signaling pathways, which increases the expression of proinflammatory mediators (Noguchi, 2008).

In this study, effects of SEP-2 on intracellular ROS levels in macrophages were detected with DCHF-DA staining by flow cytometric analysis. As shown in Fig. 4a, compared to the control group, the mean fluorescence signal was noticeably right-shifted after treatment with different concentrations of SEP-2. The quantification (Fig. 4b) revealed that fluorescence intensity dose-dependently increased when Raw264.7 cells were stimulated with 100–800 μg/mL SEP-2, thus demonstrating the upregulation of intracellular ROS production was mediated by SEP-2 treatment. This result may be partly explained by the increased NO level

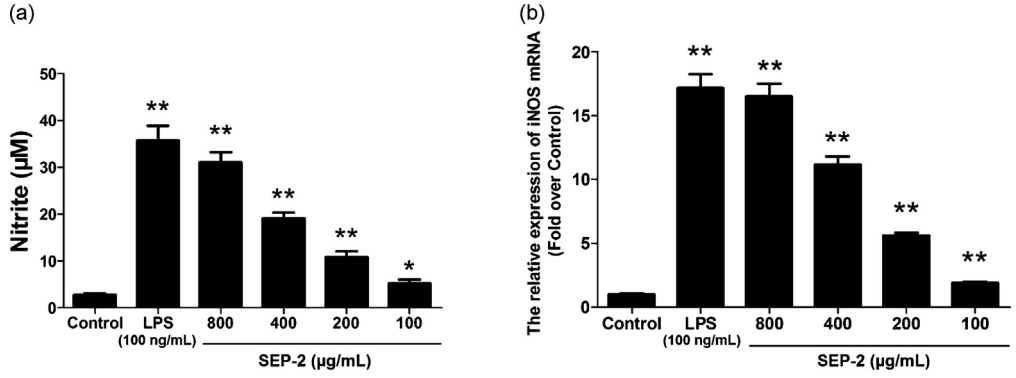

Fig. 3. Effects of SEP-2 on NO generation and iNOS mRNA expression. (a) RAW264.7 cells were treated with various concentrations of SEP-2 for 24 h. The nitrite concentration in the supernatant was detected by Griess reaction. LPS (100 ng/mL) was used as positive control. Values are expressed as mean ± SD ($n = 3$). $^{*}p < 0.05$, $^{**}p < 0.01$ compared with control group. (b) RAW264.7 cells were treated with various concentrations of SEP-2 for 12 h. The levels of iNOS mRNA were determined by RT-PCR analysis. LPS (100 ng/mL) was used as positive control. Values are expressed as mean ± SD ($n = 3$). $^{*}p < 0.05$, $^{**}p < 0.01$ compared with control group.

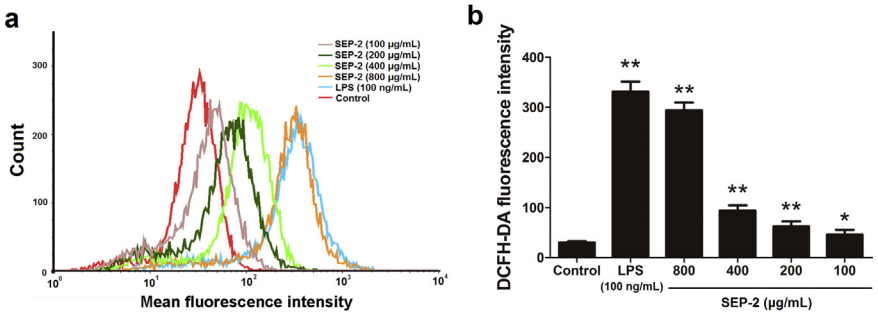

Fig. 4. Effects of SEP-2 on intracellular ROS level. (a) RAW264.7 cells were treated with various concentrations of SEP-2 for 24 h. The cells were stained with 10 μM DCFH-DA and analyzed using flow cytometric analyses. LPS (100 ng/mL) was used as positive control. (b) Bar graphs showing the mean fluorescence intensity. Values are expressed as mean ± SD ($n = 3$). $^{*}p < 0.05$, $^{**}p < 0.01$ compared with control group.

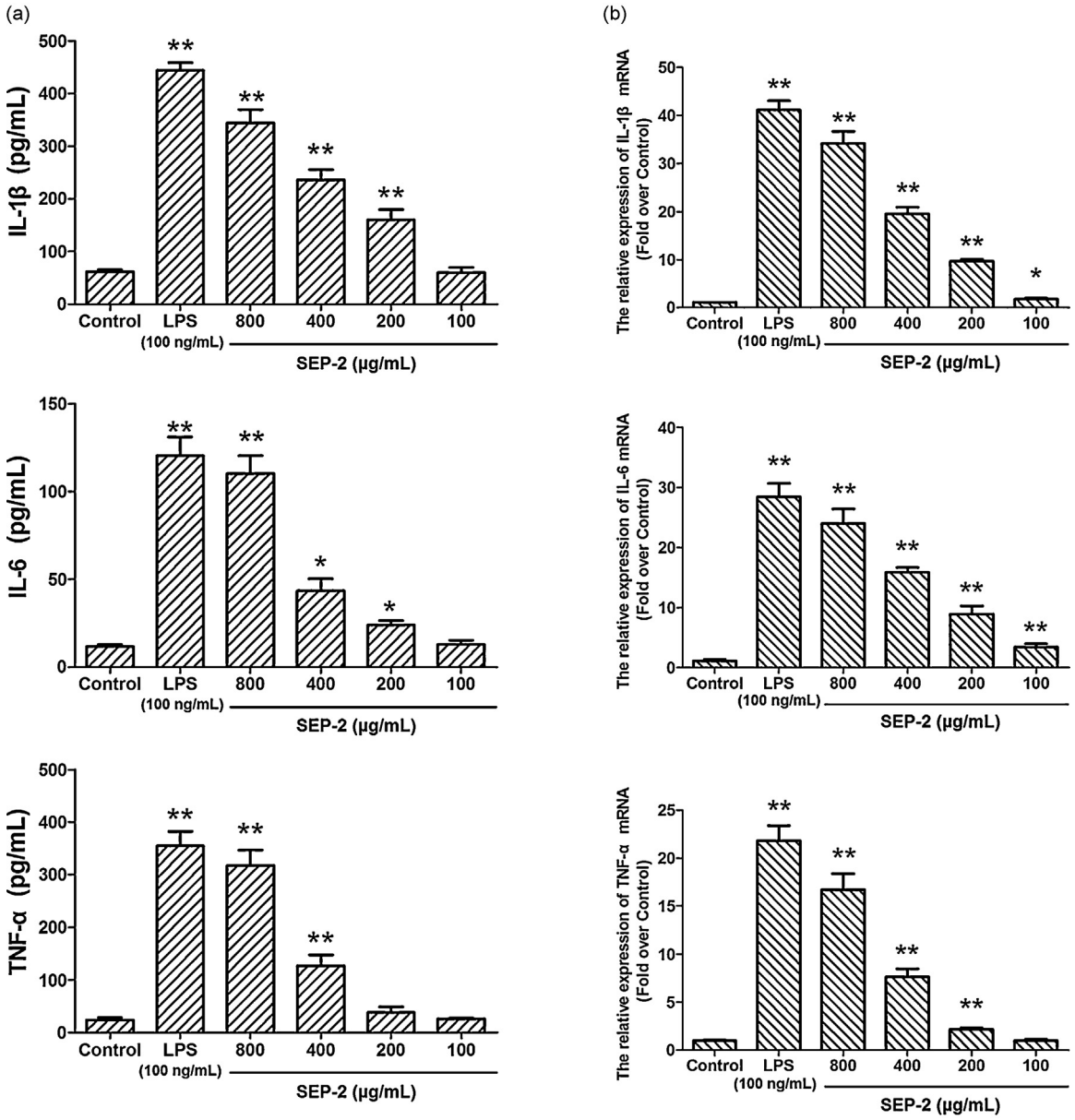

Fig. 5. Effects of SEP-2 on IL-1β, IL-6, and TNF-α secretion and mRNA expression. (a) RAW 264.7 cells were incubated with indicated concentrations of SEP-2 for 24 h, IL-1β, IL-6 and TNF-α in cell lysates were analyzed by ELISA. LPS (100 ng/mL) was used as positive control. Values are expressed as mean ± SD ($n = 3$). $^{*}p < 0.05$, $^{**}p < 0.01$ compared with control group. (b) RAW 264.7 cells were incubated with indicated concentrations of SEP-2 for 12 h, mRNA levels of IL-1β, IL-6 and TNF-α were analyzed by RT-PCR analysis. LPS (100 ng/mL) treated cells were used as positive control. Values are expressed as mean ± SD ($n = 3$). $^{*}p < 0.05$, $^{**}p < 0.01$ compared with control group.

caused by SEP-2 treatment. The surplus NO competed with oxygen causing the displacement of oxygen from cytochrome *c* oxidase, leading to a limitation in the rate of transfer in the electron transport chain, which resulted in the generation of ROS (O'Neill & Hardie, 2013).

3.3.3. SEP-2 positively regulates the transcription and secretion of proinflammatory cytokines

Activated macrophages could generate and sequentially secrete a variety of proinflammatory cytokines such as TNF-α, IL-1β and IL-6. These cytokines have a broad range of biological activities, particularly in the inflammatory and immune responses (Lee & Hong, 2011).

To evaluate the effect of SEP-2 on inflammatory cytokines secretion in RAW264.7 macrophages, ELISA assays were applied to measure TNF-α, IL-1β and IL-6 levels in culture supernatants of RAW264.7 cells treated by various concentrations of SEP-2 (100, 200, 400 and 800 μg/mL) for 24 h. The results revealed that the secretion of IL-1β, IL-6 and TNF-α significantly increased from 59.44, 12.81, 26.00 pg/mL to 343.56, 110.12, 317.36 pg/mL, respectively (Fig. 5a), suggesting that SEP-2 enhances the secretion of IL-1β, IL-6 and TNF-α in a dose-dependent manner. Furthermore, to investigate whether the effect of SEP-2 on the production of IL-1β, IL-6 and TNF-α occurred at the level of gene expression, mRNA levels of these cytokines were determined by RT-PCR. As shown in Fig. 5b, consistent with the ELISA results, the mRNA expression of IL-1β, IL-6 and TNF-α increased dose-dependently (by 34.12-, 24.01- and 16.68-fold respectively) compared to the control group. These results strongly indicate that SEP-2 promotes the expression and secretion of inflammatory cytokines in RAW264.7 macrophages.

The heterogeneity in macrophage phenotypes has given place to its classification as M1 and M2 phenotypes corresponding to classically and alternatively activated macrophages, respectively (Barros, Hauck, Dreyer, Kempkes, & Niedobitek, 2013). The pro-inflammatory M1 state induced by LPS and interferon-γ is characterized by increased level of TNF-α, IL-1, IL-6, IL-23, and ROS, while the anti-inflammatory M2 state triggered by IL-4 and IL-13 upregulates scavenger, mannose, galactose receptors and IL-1 receptor antagonist and downregulates IL-1β and other proinflammatory cytokines (Davis et al., 2013).

In this work, we demonstrated that SEP-2 significantly enhanced ROS level, NO production and inflammatory cytokines secretion including IL-1β, IL-6, and TNF-α, which was similar to the M1 macrophage profile indicating SEP-2 might induce macrophage activation through the polarization toward M1 state. Available literatures suggest that classically activated M1 macrophages are potent effector cells integrated in Th1 responses, which are responsible for killing invading pathogens and tumor cells and produce copious amounts of proinflammatory cytokines (Diaz-Gandarilla, Osorio-Trujillo, Hernandez-Ramirez, & Talamas-Rohana, 2013; Nieuwenhuizen et al., 2014; Syed & Bhandari, 2013). Thus it is predictable that SEP-2 probably have the capability to enhance the microbicidal activity and killing function of macrophages. It would be informative to better understand the molecular pathways by which SEP-2 activate the macrophages and make further research on the functional studies of SEP-2 in animal models.

4. Conclusion

In the present study, the extraction process of SEP-2 was optimized by RSM with a three-variable, three-level BBD. The optimal extraction parameters were as follows: extraction temperature of 81.6 °C, extraction time of 5.09 h, and an ethanol to supernatant ratio of 4.83:1. Under these optimized conditions, SEP-2 content in crude polysaccharide was 23.21 ± 0.14%, showing no significant difference compared to the predicted value (23.117%). After purification by cellulose DE52 (OH^-) anion exchange and Sephacryl S-400 column chromatography, SEP-2 was established to be a D-glucan composed of (1 → 4)-linked D-Glcp backbone with (1 → 3)-D-Glcp side chains and a molecular weight of 6.78×10^5 Da. Investigation of the immunostimulatory effect of SEP-2 on murine macrophage cell line RAW264.7 revealed that SEP-2 significantly upregulates the production of NO, intracellular ROS and the secretion of inflammatory cytokines including IL-1β, IL-6 and TNF-α. Based on these lines of evidence, SEP-2 has the potential to increase the macrophage functions by inducing macrophage activation through the polarization toward M1 state. Detailed mechanism and convincing functional studies in animal models should be further investigated.

Appendix A. Supplementary data

Supplementary data associated with this article can be found, in the online version, at http://dx.doi.org/10.1016/j.carbpol.2014.04.010.

References

Barros, M. H., Hauck, F., Dreyer, J. H., Kempkes, B., & Niedobitek, G. (2013). Macrophage polarisation: An immunohistochemical approach for identifying M1 and M2 macrophages. *PLoS ONE*, *8*(11), e80908.

Bi, H., Ni, X., Liu, X., Iteku, J., Tai, G., Zhou, Y., et al. (2009). A novel water-soluble β-(1 → 6)-D-glucan isolated from the fruit bodies of *Bulgaria inquinans* (Fries). *Carbohydrate Research*, *344*(10), 1254–1258.

Cheng, A., Wan, F., Wang, J., Jin, Z., & Xu, X. (2008). Macrophage immunomodulatory activity of polysaccharides isolated from *Glycyrrhiza uralensis* fish. *International Immunopharmacology*, *8*(1), 43–50.

Chihara, G. (1992). Recent progress in immunopharmacology and therapeutic effects of polysaccharides. *Developments in Biological Standardization*, *77*, 191.

Ciucanu, I., & Kerek, F. (1984). A simple and rapid method for the permethylation of carbohydrates. *Carbohydrate Research*, *131*(2), 209–217.

Cordeiro, L. M. C., Reinhardt, V. D. F., & Iacomini, M. (2012). Glucomannan and branched (1 → 3)(1 → 6) β-glucan from the aposymbiotically grown *Physcia kalbii* mycobiont. *Phytochemistry*, *84*, 88–93.

Davis, M. J., Tsang, T. M., Qiu, Y., Dayrit, J. K., Freij, J. B., Huffnagle, G. B., et al. (2013). Macrophage M1/M2 polarization dynamically adapts to changes in cytokine microenvironments in *Cryptococcus neoformans* infection. *MBio*, *4*(3), e00264-00213

Devi, K. S. P., Roy, B., Patra, P., Sahoo, B., Islam, S. S., & Maiti, T. K. (2013). Characterization and lectin microarray of an immunomodulatory heteroglucan from *Pleurotus ostreatus mycelia*. *Carbohydrate Polymers*, *94*(2), 857–865.

Diaz-Gandarilla, J. A., Osorio-Trujillo, C., Hernandez-Ramirez, V. I., & Talamas-Rohana, P. (2013). PPAR activation induces M1 macrophage polarization via cPLA(2)-COX-2 inhibition, activating ROS production against *Leishmania mexicana*. *BioMed Research International*, *2013*, 215283.

Drapier, J. C., & Hibbs, J. B., Jr. (1988). Differentiation of murine macrophages to express nonspecific cytotoxicity for tumor cells results in L-arginine-dependent inhibition of mitochondrial iron–sulfur enzymes in the macrophage effector cells. *Journal of Immunology*, *140*(8), 2829–2838.

Fisher, R. A. (1922). On the interpretation of χ^2 from contingency tables, and the calculation of P. *Journal of the Royal Statistical Society*, *85*(1), 87–94.

Granger, D. L., Taintor, R. R., Boockvar, K. S., Hibbs, J., & John, B. (1995). Determination of nitrate and nitrite in biological samples using bacterial nitrate reductase coupled with the Griess reaction. *Methods*, *7*(1), 78–83.

Jiang, Z., Okimura, T., Yamaguchi, K., & Oda, T. (2011). The potent activity of sulfated polysaccharide, ascophyllan, isolated from *Ascophyllum nodosum* to induce nitric oxide and cytokine production from mouse macrophage RAW264.7 cells: Comparison between ascophyllan and fucoidan. *Nitric Oxide*, *25*(4), 407–415.

Kadowaki, T., Ohno, S., Taniguchi, Y., Inagawa, H., Kohchi, C., & Soma, G. (2013). Induction of nitric oxide production in RAW264.7 cells under serum-free conditions by O-antigen polysaccharide of lipopolysaccharide. *Anticancer Research*, *33*(7), 2875–2879.

Kroncke, K. D., Fehsel, K., Schmidt, T., Zenke, F. T., Dasting, I., Wesener, J. R., et al. (1994). Nitric oxide destroys zinc–sulfur clusters inducing zinc release from metallothionein and inhibition of the zinc finger-type yeast transcription activator LAC9. *Biochemical and Biophysical Research Communications*, *200*(2), 1105–1110.

Kumirska, J., Szafranek, J., Czerwicka, M., Gołębiowski, M., Paszkiewicz, M., Dziadziuszko, H., et al. (2008). Smith degradation of the O-antigenic polysaccharide of *Salmonella* Dakar: Structural studies of the products. *Carbohydrate Research*, *343*(6), 1120–1125.

Lee, I. T., & Yang, C. M. (2012). Role of NADPH oxidase/ROS in pro-inflammatory mediators-induced airway and pulmonary diseases. *Biochemical Pharmacology*, *84*(5), 581–590.

Lee, J. S., & Hong, E. K. (2011). Immunostimulating activity of the polysaccharides isolated from *Cordyceps militaris*. *International Immunopharmacology*, *11*(9), 1226–1233.

Li, Y. H., Yan, Z. Q., Brauner, A., & Tullus, K. (2002). Activation of macrophage nuclear factor-kappa B and induction of inducible nitric oxide synthase by LPS. *Respiratory Research*, *3*, 23.

Liu, C., Lin, Q., Gao, Y., Ye, L., Xing, Y., & Xi, T. (2007). Characterization and antitumor activity of a polysaccharide from *Strongylocentrotus nudus* eggs. *Carbohydrate Polymers*, *67*(3), 313–318.

Liu, C., Xi, T., Lin, Q., Xing, Y., Ye, L., Luo, X., et al. (2008). Immunomodulatory activity of polysaccharides isolated from *Strongylocentrotus nudus* eggs. *International Immunopharmacology*, *8*(13–14), 1835–1841.

Meena, D., Das, P., Kumar, S., Mandal, S., Prusty, A., Singh, S., et al. (2013). Beta-glucan: An ideal immunostimulant in aquaculture (a review). *Fish Physiology and Biochemistry*, *39*(3), 431–457.

Nieuwenhuizen, L., Schutgens, R. E., Coeleveld, K., Mastbergen, S. C., Roosendaal, G., Biesma, D. H., et al. (2014). Hemarthrosis in hemophilic mice results in alterations in M1-M2 monocyte/macrophage polarization. *Thrombosis Research*, *133*(3), 390–395.

Noguchi, T. (2008). ROS-dependent activation of ASKI in inflammatory signaling. *Journal of Oral Biosciences*, *50*(2), 107–114.

O'Neill, L. A., & Hardie, D. G. (2013). Metabolism of inflammation limited by AMPK and pseudo-starvation. *Nature*, *493*(7432), 346–355.

Ramberg, J. E., Nelson, E. D., & Sinnott, R. A. (2010). Immunomodulatory dietary polysaccharides: A systematic review of the literature. *Nutrition Journal*, *9*, 54.

Richter, C., Gogvadze, V., Schlapbach, R., Schweizer, M., & Schlegel, J. (1994). Nitric-oxide kills hepatocytes by mobilizing mitochondrial calcium. *Biochemical and Biophysical Research Communications*, *205*(2), 1143–1150.

Santana-Filho, A. P., Noleto, G. R., Gorin, P. A. J., de Souza, L. M., Iacomini, M., & Sassaki, G. L. (2012). GC–MS detection and quantification of lipopolysaccharides in polysaccharides through 3-O-acetyl fatty acid methyl esters. *Carbohydrate Polymers*, *87*(4), 2730–2734.

Schepetkin, I. A., & Quinn, M. T. (2006). Botanical polysaccharides: Macrophage immunomodulation and therapeutic potential. *International Immunopharmacology*, *6*(3), 317–333.

Schepetkin, I. A., Xie, G., Kirpotina, L. N., Klein, R. A., Jutila, M. A., & Quinn, M. T. (2008). Macrophage immunomodulatory activity of polysaccharides isolated from *Opuntia polyacantha*. *International Immunopharmacology*, *8*(10), 1455–1466.

Schmittgen, T. D., & Livak, K. J. (2008). Analyzing real-time PCR data by the comparative C_T method. *Nature Protocols*, *3*(6), 1101–1108.

Syed, M. A., & Bhandari, V. (2013). Hyperoxia exacerbates postnatal inflammation-induced lung injury in neonatal BRP-39 null mutant mice promoting the M1 macrophage phenotype. *Mediators of Inflammation*, *2013*, 457189.

Wang, C. L., Lu, C. Y., Pi, C. C., Zhuang, Y. J., Chu, C. L., Liu, W. H., et al. (2012). Extracellular polysaccharides produced by *Ganoderma formosanum* stimulate macrophage activation via multiple pattern-recognition receptors. *BMC Complementary and Alternative Medicine*, *12*(1), 119.

Wang, H., Wang, M., Chen, J., Tang, Y., Dou, J., Yu, J., et al. (2011). A polysaccharide from *Strongylocentrotus nudus* eggs protects against myelosuppression and immunosuppression in cyclophosphamide-treated mice. *International Immunopharmacology*, *11*(11), 1946–1953.

Wang, M., Wang, H., Tang, Y., Kang, D., Gao, Y., Ke, M., et al. (2011). Effective inhibition of a *Strongylocentrotus nudus* eggs polysaccharide against hepatocellular carcinoma is mediated via immunoregulation *in vivo*. *Immunology Letters*, *141*(1), 74–82.

Zhang, L., Koyyalamudi, S. R., Jeong, S. C., Reddy, N., Bailey, T., & Longvah, T. (2013). Immunomodulatory activities of polysaccharides isolated from *Taxillus chinensis* and *Uncaria rhyncophylla*. *Carbohydrate Polymers*, *98*(2), 1458–1465.